

Development of Advanced Pellet Injector Systems for Plasma Fueling^{*)}

Ryuichi SAKAMOTO, Hiroshi YAMADA and LHD experimental group

National Institute for Fusion Science, Toki, Gifu 509-5292, Japan

(Received 21 August 2008 / Accepted 25 November 2008)

Two types of solid hydrogen pellet injection systems have been developed, and plasma refueling experiments have been performed using these pellet injectors. One is an *in-situ* pipe-gun type pellet injector, which has the simplest design of all pellet injectors. This *in-situ* pipe-gun injector has 10 injection barrels, each of which can independently inject cylindrical solid hydrogen pellets (3.4 and 3.8 mm in diameter and length, respectively) at velocities up to 1,200 m/s. The other is a repetitive pellet injector with a screw extruder, which can form a 3.0 mm ϕ solid hydrogen rod continuously at extrusion rates up to 55 mm/s. This extruder allows consecutive pellet injection up to 11 Hz without time limit. Both of these pellet injectors employ compact cryo-coolers to solidify hydrogen; therefore, they can be operated using only electrical input instead of a complicated liquid helium supply system. In particular, using a combination of the repetitive pellet injector with cryo-coolers provides a steady-state capability with minimum maintenance.

© 2009 The Japan Society of Plasma Science and Nuclear Fusion Research

Keywords: solid hydrogen pellet, fueling, cryo-cooler, pellet injector, steady state operation

DOI: 10.1585/pfr.4.002

1. Introduction

Core fueling will play a primary role in future fusion reactors in which magnetically confined burning plasma can be sustained by its own α particle heating. Gas puffing, which provides fuel particles by blowing neutral gas onto a plasma surface, has been typically used for fueling high-temperature plasma in toroidal magnetic fusion research. However, its capability is limited in large-scale high-temperature plasmas, since a thick, hot scrape-off layer prevents penetration of the neutrals, and the particles cannot be provided efficiently to the core plasma. Pellet injection, which injects cryogenic hydrogen pellets into the core plasma directly at high speeds (typically more than 1,000 m/s), is cited as an alternative means of efficient core fueling. Pellet injection has been investigated since the past thirty years [1–3], and many studies have indicated that pellet injection contributes to not only efficient fueling but also improvements in plasma confinement properties. In addition, the pellet injection has merits that become significant in a fusion reactor. High-efficiency core fueling enables minimization of the amount of tritium to be used, and it may reduce the tritium inventory in a vacuum vessel. Pellet injection can provide fuel particles to the core plasma with negligible energy requirements compared with other core fueling options, such as neutral beam injection (NBI). Despite these advantages, the pellet injection is not included in the infrastructure facilities due to its limited use in present plasma experiments and technolog-

ical difficulties. In order to operate the pellet injector system as an infrastructure facility for plasma experiments, a highly reliable and stable system is required. One of the major difficulties in the current pellet injector system is the use of liquid helium for hydrogen solidification. The liquid helium usage causes reduction in the utilization rate due to the need for its replenishment. Use of a closed-cycle helium refrigerator is a valid solution [4], but it becomes a relatively large facility requiring considerable maintenance and reduction in operational flexibility.

From the perspective of fueling for fusion reactors, demonstration of steady-state pellet injection is essential. Several research groups have already developed repetitive pellet injectors that use prepared solid hydrogen in advance of the pellet injections. Plasma experiments with repetitive pellet injections have been conducted on JET [5], ASDEX-upgrade [6], DIII-D [7], and JT-60U [8, 9]. These injectors perform adequately for previous plasma experiments, but are inadequate for fueling a fusion reactor due to the limited quantity of solid hydrogen production. We have developed pellet injection as one of the infrastructure facilities not only for existing plasma experiments but also for future fusion reactors. Highly reliable pellet injectors for stable operation have been developed, and many successive improvements have been made. The first pellet injector that we have developed is a conventional *in-situ* pipe-gun type pellet injector [10], and the second is a repetitive pellet injector with steady-state, low-maintenance injection capability [11]. Both injectors employ compact cryo-coolers, which enable stable operation in absence of liquid helium.

author's e-mail: sakamoto@LHD.nifs.ac.jp

^{*)} This article is based on the invited talk at the 24th JSPF Annual Meeting (2007, Himeji).

In particular, using a combination of the repetitive pellet injector with cryo-coolers provides a steady-state capability with minimum maintenance.

In this paper, two pellet injectors developed at the National Institute for Fusion Science (NIFS) are described. The repetitive pellet injector is described in detail.

2. *in-situ* Pipe-Gun Type Pellet Injector

In order to produce a solid hydrogen pellet, a very low temperature below the triple point (13.9 K for H₂, 18.7 K for D₂, 20.6 K for T₂ [12]) is required. Liquid helium cooling has been employed in all previous pellet injectors. Here, we employ Gifford-McMahon cycle compact cryo-coolers (SHI SRDK-415D), which utilizes electrical input only instead of liquid helium as new initiative in the world.

First, we developed a conventional *in-situ* pipe-gun type pellet injector in order to examine the adequacy of pellet injection for fueling high-temperature plasmas. In the *in-situ* pipe-gun concept, a solid hydrogen pellet is directly formed in an injection barrel, and then pneumatically accelerated by high-pressure propellant gas [13]. As there are no moving parts in this cryogenic system, stable and reliable operation is possible. Although the *in-situ* pipe-gun concept basically can inject a single pellet, this injector can inject 10 pellets using 10 parallel injection barrels.

Combination of the compact cryo-cooler and *in-situ* pipe-gun concept results in stable and reliable operation. The pellet injector has demonstrated stable and reliable performance on the Large Helical Device (LHD) during the 11 year experimental project. The experimental results indicated the efficacy of the pellet injection not only for

efficient fueling but also for plasma confinement improvement [14].

3. Development of Repetitive Pellet Injector

Improvements of plasma confinement properties by means of pellet fueling were reported in many previous studies [1, 15]. However, these improvements were transient and the sustainability of good plasma confinement properties has to demonstrate in order to extrapolate the scenarios to a fusion reactor. We have developed a reactor-oriented repetitive pellet injector with steady-state operation capability. Its key design features are as follows:

- Cooling by compact cryo-coolers: The pellet injector is operated using electrical input only, which is the most fundamental facility in a laboratory, instead of a complicated liquid helium supply system. This design enables flexible and reliable operation.
- Screw extruder for solid hydrogen production: The Screw-extruder can produce solid hydrogen rod via simultaneous replenishment, liquefaction, and solidification of hydrogen gas. This design enables steady-state operation in principle.
- Pneumatic pipe-gun pellet acceleration: This design enables reliable and reproducible pellet injection with easy injection-timing control.

A system diagram of the repetitive pellet injector is shown in Fig. 1. The repetitive pellet injector consists of a gas supply system, a cryo system and a differential pumping system. All control objects (contact I/O, ~100 ch;

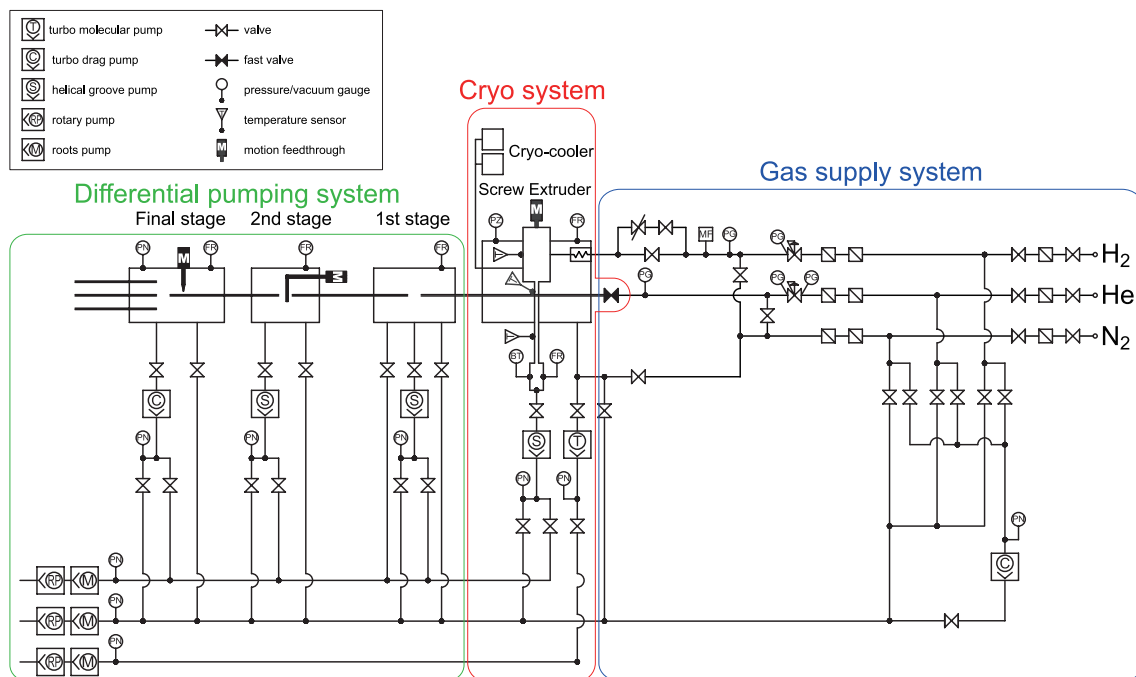


Fig. 1 System diagram of the repetitive pellet injector.

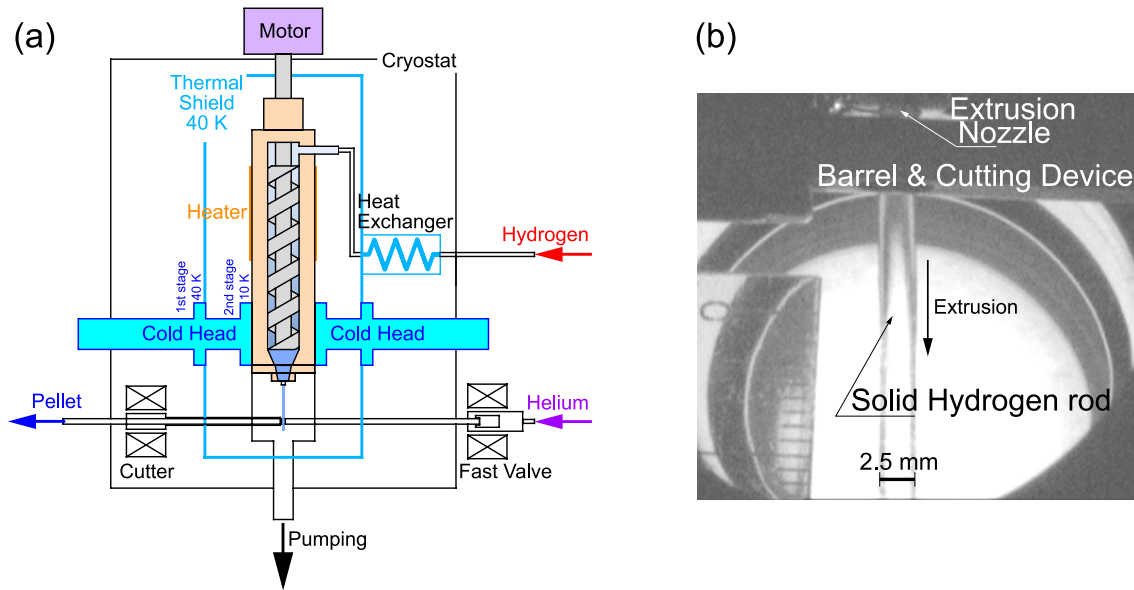


Fig. 2 (a) Conceptual drawing of the screw extruder and (b) photograph of the extruded solid hydrogen rod.

analog I/O, ~30 ch) can be operated remotely, and automatically using a programmable logical controller (PLC) placed in the experimental hall. An operator can give directions to the PLC via a TCP/IP-based network using a graphical user interface program on a Windows-based PC placed in the control room.

3.1 Solid hydrogen extrusion with screw extruder

In the previous solid hydrogen extruder, such as the ORNL extruder [16], solid hydrogen is formed in the cryo-cylinder in advance, and then it is extruded from a nozzle by pressurizing with a piston. The usable amount of solid hydrogen is restricted by the capacity of the cryo-cylinder and the time required in preparing successive batches of solid hydrogen. On the other hand, the screw extrusion concept, which was proposed by Mitsubishi Heavy Industry [17] and developed by PELIN Laboratory [18, 19], can produce a solid hydrogen rod continuously. We adopted the screw extrusion concept as a key design of the repetitive pellet injector. A conceptual drawing of the screw extruder is shown in Fig. 2(a). Making use of our previous experience on pellet injector development, we employed two Gifford-McMahon cycle 4 K cryo-coolers to cool the cryo-cylinder. The total cooling capacity of the cryo-coolers is 20 W at 8 K. The lower part of a copper cryo-cylinder, which has a built-in screw, is connected to the second stage of the cold heads of two cryo-coolers, and the cryo-cylinder is cooled to below 6 K in the standby phase. In order to prevent heat radiation, the cryo-cylinder is surrounded by a copper thermal shield, which is cooled to 40 K by the first stage of the cold heads of the cryo-coolers. The cooling rate of the screw extruder is about ~1.0 K/min, and it takes 4 hour to cool down from room

temperature to operational temperature.

Hydrogen gas is pre-cooled in a heat exchanger at the same temperature with the thermal shield, and then flows into the copper cryo-cylinder that has a built-in rotating screw. The pre-cooled hydrogen gas is further cooled in the cryo-cylinder to be liquefied and solidified, while the solid hydrogen rod is extruded by the rotating screw from a nozzle (Fig. 2 (b)). The diameter of the solid hydrogen rod is selectable as 2.5 mm or 3.0 mm by changing the nozzle size. Since the screw extruder can extrude the solid hydrogen rod simultaneously with replenishment, liquefaction, and solidification of hydrogen, it can operate continuously. The solid hydrogen extrusion speed, which is measured by extruding length at a given time is proportional to the screw rotational speed, as shown in Fig. 3. The maximum extrusion speed is 55 mm/s at 37.5 rpm of screw rotation for a 3 mm ϕ solid hydrogen rod, and this value corresponds to 34 mg/s and 40 Pa m³/s for H₂ in the other units. The extrusion speed is sufficient for fueling for LHD discharges, and it has already achieved 40% of ITER pellet fueling requirements [20, 21]. When the extrusion speed becomes over speed, the solid hydrogen melts due to temperature rise and is abruptly dumped from the nozzle. In order to increase the throughput of the solid hydrogen, sufficient cooling capacity and/or reduction of frictional heat generation are required. Synchronous control of the multiple extruders is another sure method to increase the throughput of the solid hydrogen. And this method has substantial merit from the view point of fault redundancy.

The operating temperature range of the screw extruder is from 9.5 to 13.0 K. The screw extruder temperature is maintained above 10 K using an electric heater during operation in order to prevent damage to the rotating screw from cryogenically hardened solid hydrogen. The upper

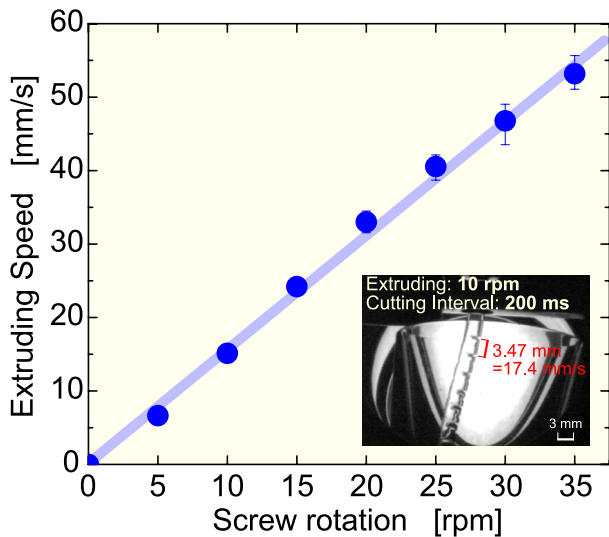


Fig. 3 Solid hydrogen extrusion speed versus screw rotational speed. The image shows an example of the solid hydrogen extrusion speed measurement. The marking on the solid hydrogen rod is made using a cutting device, which operates at regular time intervals.

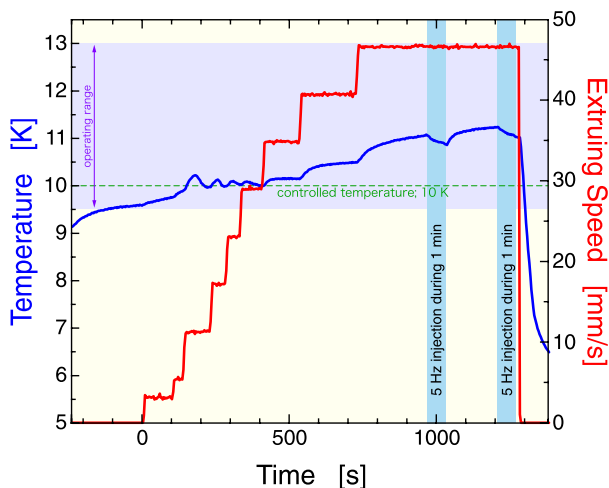


Fig. 4 The screw extruder temperature rise during operation with a stepwise change of extrusion speed. The operational temperature ranges from 9.5 to 13 K. Extruded solid hydrogen sublimate in the extrusion chamber during extrusion, which lead to degradation of the vacuum insulation. On the other hand, the vacuum insulation is recovered at the pellet injection periods which is indicated by blue hatching around $t = 1,000$ s and $t = 1,250$ s.

temperature limit is determined by the melting temperature of solid hydrogen. Friction and deformation of the solid hydrogen during extrusion generate heat and may lead to temperature rise beyond the operational range, especially at high extrusion speed. Figure 4 shows the screw extruder temperature rise during operation. The extrusion speed, which is denoted by red line, was changed stepwise from

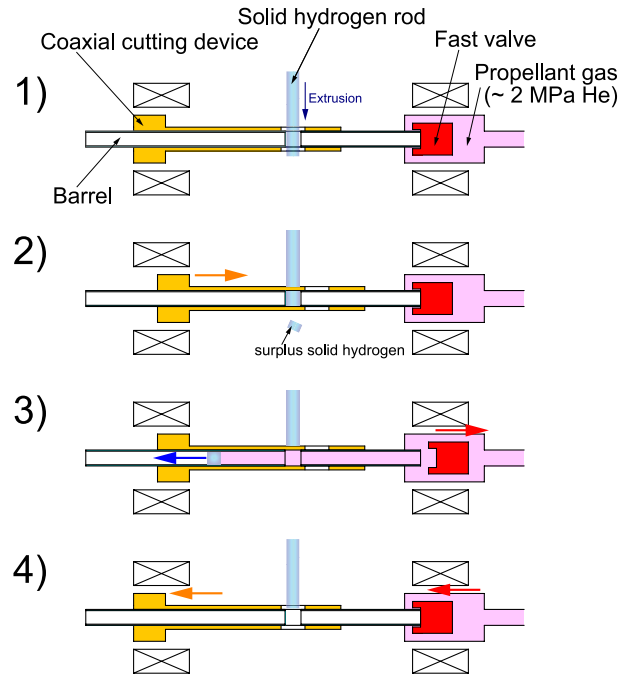


Fig. 5 A cycle of the solid hydrogen cutting and launching process.

2.5 to 46.5 mm/s. Although there is a minor temperature perturbation due to the extrusion speed change, the maximum temperature rise from a preset temperature (10 K) is less than 0.2 K up to 35 mm/s, which corresponds to more than 10 pellets per second. If the extrusion speeds exceed 35 mm/s, the temperature rise becomes discernible and reaches 11.2 K at 46 mm/s; however, the rising temperature saturates at a value that is sufficiently low compared with the maximum operating temperature.

A noteworthy finding is the temperature drop during pellet injection phases, despite a constant extrusion speed phase, as denoted by the blue zones in Fig. 4. Extruded solid hydrogen is evaporated on contact with the vacuum chamber, which results in pressure increase above 0.1 Pa, which is insufficient for vacuum insulation. On the other hand, the vacuum chamber pressure becomes better, and vacuum insulation recovers during the pellet injection phases because extruded solid hydrogen is ejected from the chamber. The temperature drop is assumed to be related to vacuum insulation. This suggests the importance of maintaining sufficient vacuum insulation, which, however, is not significant in the actual operation because the formed solid hydrogen is cut and launched in real time, as described in Sec. 3.2.

3.2 Pellet cut and launch

Extruded solid hydrogen rod needs to be cut into a pellet form with the proper size before injection. Solid hydrogen rod cutting and pneumatic pellet acceleration are simultaneously performed as shown in Fig. 5, using a

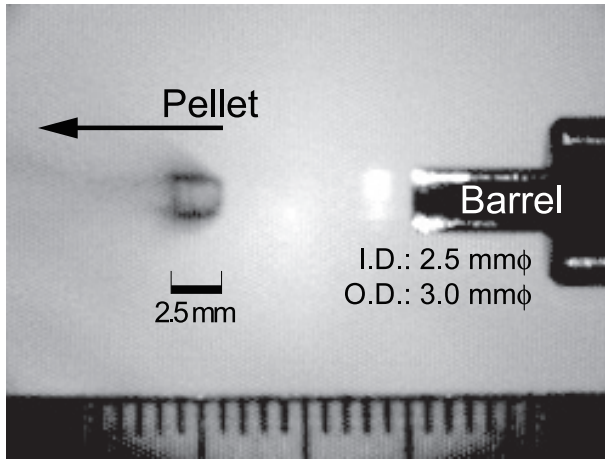


Fig. 6 Typical shadowgraph image of a pellet using 180 ns pulse light source at the muzzle of a barrel. The pellet velocity is around 400 m/s.

solenoid operated coaxial cutting device and a fast valve.

- 1) At the ready position, a pair of holes of the coaxial cutting device coincides with holes in the injection barrel. Solid hydrogen rod from an extrusion nozzle can go down through the holes.
- 2) When a pellet is launched, the coaxial cutting device slides along the barrel to cut and load the solid hydrogen pellet. At the same time, the holes in the barrel are hermetically sealed by the inner wall of the coaxial cutting device. Surplus solid hydrogen drops down to an evaporator and evaporates as hydrogen gas.
- 3) 10 ms after the solid hydrogen cutting, the fast valve opens and high-pressure propellant gas (typically He gas) surges into the barrel. The solid hydrogen pellet is accelerated by expansion of the propellant gas.
- 4) After injection, the coaxial cutting device and fast valve return to the ready position, and the solid hydrogen rod resumes moving into the barrel. The injector waits for the next injection trigger.

The above-mentioned real-time cutting and pneumatic launch procedures with the screw extruder enable steady pellet injections with a maximum repetitive frequency of 11 Hz. Stable 10,000 pellet injection at 10 Hz has been demonstrated without restriction on further long-duration injection. Figure 6 shows the shadowgraph image of the accelerated pellet at a muzzle of the barrel. The pellet mass, which is estimated from the image size coupled with the pellet three-dimensional shape, is 5.1×10^{20} atoms for a 2.5 mm pellet and 8.8×10^{20} atoms for a 3.0 mm pellet. The screw extruder can provide more than 15 pellets of solid hydrogen per second even when considering 20% loss at cutting. However, the pellet injection repetitive frequency is limited to 11 Hz by the cutting process because insufficient moving velocity of the cutting device interferes with the solid hydrogen rod movement into the barrel.

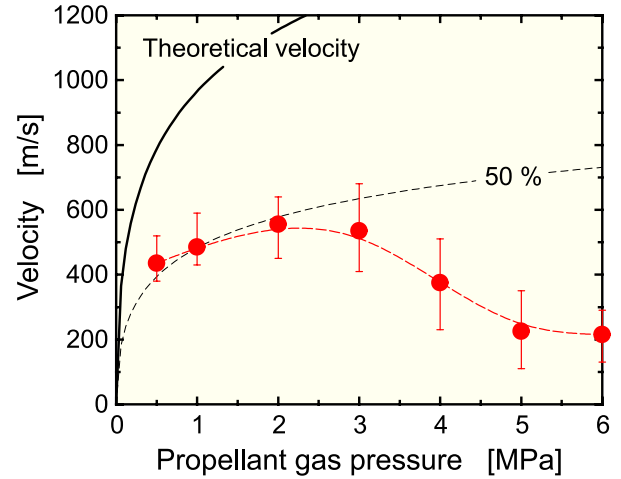


Fig. 7 Dependence of the pellet velocity on propellant gas pressure.

The pellet size can be adjusted by changing the ratio of the extrusion speed to the injection frequency. Assuming that the extrusion speed is sufficiently high compared with the injection frequency, the injected pellet becomes a definite size, which is determined by the diameters of the injection barrel and solid hydrogen rod, while increasing surplus solid hydrogen with the extrusion speed rise. Assuming that the extrusion speed is insufficient compared with the injection frequency, solid hydrogen is cut off before reaching the rated size, and undersize pellets can be injected. Under such circumstances, the pellet mean size is proportional to the extrusion speed under the constant injection frequency condition. At the same time, variation in the pellet size and velocity becomes large.

The propellant gas pressure dependence on pellet velocity is shown in Fig. 7. Measured and theoretically predicted pellet velocities are denoted by filled circles and the solid line, respectively. The theoretical velocity of the pneumatically accelerated pellet can be described by a propagation of one-dimensional rarefaction wave [22], which is known from the ideal gun theory:

$$\frac{M}{A_p} \frac{dU(t)}{dt} = P_0 \left(1 - \frac{(\gamma - 1)U(t)}{2C_0} \right)^{2\gamma/(\gamma-1)}, \quad (1)$$

where $U(t)$, M , A_p , P_0 , γ , ρ_s and C_0 denote the pellet velocity, pellet mass ($= 4\pi(d/2)^3\rho_s/3$), projected area of a pellet ($= (d/2)^2\pi$), initial pressure of propellant gas, specific heat ratio of propellant gas, solid hydrogen density and sound velocity of propellant gas ($= \sqrt{\gamma kT/m}$), respectively.

Pellet velocity $U(t)$ and distance of travel $X(t)$ from the injection timing are obtained by solving the above equation,

$$U(t) = \frac{2C_0}{\gamma - 1} \left[1 - \left(1 + \frac{(\gamma + 1)A_p P_0}{2MC_0} t \right)^{-(\gamma-1)/(\gamma+1)} \right], \quad (2)$$

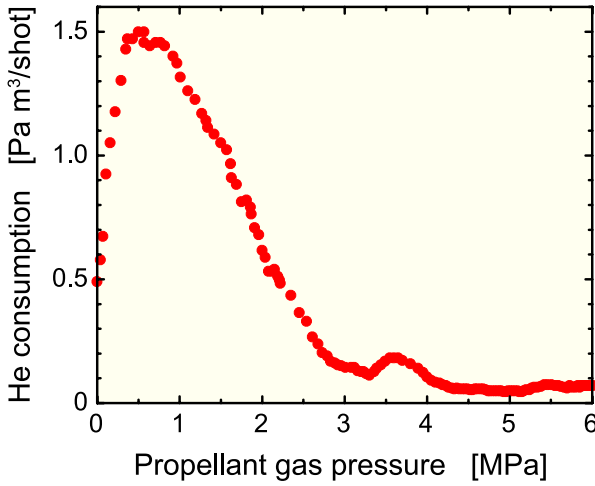


Fig. 8 Dependence of the propellant gas consumption rate on propellant gas pressure.

$$\begin{aligned}
 X(t) &= \int U(t)dt \\
 &= \frac{2C_0}{\gamma-1} \left[t - \frac{MC_0}{A_p P_0} \left(1 + \frac{(\gamma+1)A_p P_0}{2MC_0} t \right)^{2/(\gamma+1)} \right] \\
 &\quad + \frac{2MC_0^2}{(\gamma-1)A_p P_0}. \quad (3)
 \end{aligned}$$

The pellet muzzle velocity at barrel length L_0 as a function of a propellant gas pressure P_0 is obtained by substituting L_0 for $X(t)$ and eliminating t from Eqs. (2) and (3).

The measured pellet velocity is less than half of the ideal gun theory prediction. There is a positive dependence between the propellant gas pressure and pellet velocity in the ideal gun theory, but the measured velocity has a negative dependence on the propellant gas pressure above 3 MPa. The discrepancy between the prediction and measurement is caused by an effective pressure decrease due to insufficient propellant gas, because a self-regulated fast valve is employed in our pellet injector system in order to mitigate the gas load to the differential pumping system even at a high repetitive injection rate. Figure 8 shows propellant gas consumption per pellet injection at the fast valve. The gas consumption amount reaches its highest value (1.5 Pa m³/shot) at 0.5 MPa and decreases with increasing propellant gas pressure. In particular, the gas consumption amount is small above 4 MPa. In the steady-state pneumatic injection, a sustainable balance between the gas consumption required for high-speed injection and the pumping capacity is important. In order to inject the pellet with higher speed, a high flow rate fast valve and consistent pumping capacity are required.

3.3 Differential pumping system

Since the repetitive pellet injector utilizes pneumatic acceleration, a propellant gas (He) flows into the system at the time of the pellet injection. A three-stage differential

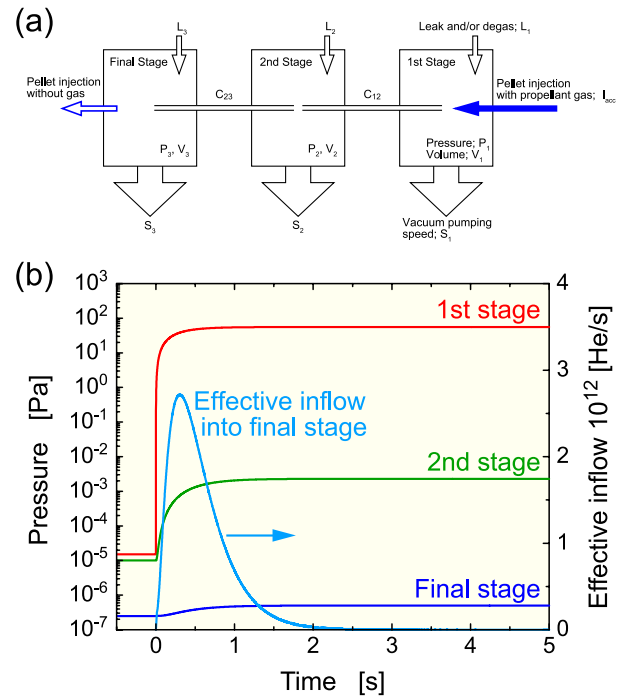


Fig. 9 (a) Conceptual diagram of the three-stage differential pumping system. (b) Propellant gas exhaust characteristic of the three-stage differential pumping system.

pumping system is employed to prevent the propellant gas from flowing into the plasma chamber. Figure 9 (a) shows a conceptual diagram of the three-stage differential pumping system. The first and the second differential pumping stages employ helical grooved vacuum pumps, which have a wide operating range from ultrahigh vacuum to the viscous flow region at pressures above 10² Pa. The performance of the three-stage differential pumping system is estimated by the following equations in the case of pellet injection at repetition rate of 10 Hz:

$$\begin{cases}
 V_1 \frac{dP_1}{dt} = I_{acc} + C_{12}(P_2 - P_1) - S_1 P_1 + L_1, \\
 V_2 \frac{dP_2}{dt} = C_{12}(P_1 - P_2) + C_{23}(P_3 - P_2) - S_2 P_2 + L_2, \\
 V_3 \frac{dP_3}{dt} = C_{23}(P_2 - P_3) - S_3 P_3 + L_3,
 \end{cases} \quad (4)$$

where I_{acc} , P_i , V_i , S_i , C_i and L_i denote the propellant gas inflow rate, pressure of the stage i , volume of the stage i , pumping capacity of the stage i , conductance between the stages i and $i+1$ (which are isolated by the guide tube), and leak and/or degassing rate of the stage i , respectively. For the sake of simplicity, the pulse gas influx due to 10 Hz pellet injection is substituted by the same amount of constant gas influx on average.

$$\left\{ \begin{array}{l} I_{\text{acc}} = 1.5 \text{ Pa m}^3 \times 10 \text{ Hz} = 15 \text{ Pa m}^3/\text{s}, \\ V_1 = 0.07 \text{ m}^3, \quad V_2 = 0.07 \text{ m}^3, \quad V_3 = 0.015 \text{ m}^3, \\ S_1 = 0.27 \text{ m}^3\text{s}^{-1}, \quad S_2 = 0.27 \text{ m}^3\text{s}^{-1}, \quad S_3 = 0.4 \text{ m}^3\text{s}^{-1}, \\ C_{12} = 1.1 \times 10^{-5} \text{ m}^3\text{s}^{-1}, \quad C_{23} = 4.3 \times 10^{-5} \text{ m}^3\text{s}^{-1}, \\ L_1 = L_2 = 1.0 \times 10^{-6} \text{ Pa m}^3\text{s}^{-1}, \quad L_3 = 1.0 \times 10^{-7} \text{ Pa m}^3\text{s}^{-1}. \end{array} \right.$$

Temporal pressure changes calculated using Eq. (4) with the above parameters is plotted in Fig. 9 (b). Since there is a direct gas influx, the vacuum at the first stage deteriorates to 10^2 Pa immediately after the start of pellet injection sequence. On the other hand, the final stage pressure is maintained reasonably low, not exceeding 10^{-6} Pa by the three-stage differential pumping. The effective inflow of the propellant gas (He) into the final stage is of the order of 10^{12} atoms per second at a maximum value, and it is lowered with the decay time constant of 1 s. Because the effective inflow is considerably small compared with the pellet mass (10^{21} atoms/s), the negative effects of the residual propellant gas are negligibly small. It is difficult to confirm experimentally the above described pumping capacity because gas evaporation from the injected pellets, which contain almost the same number of atoms as the injected propellant gas, disturbs the vacuum measurement. We confirmed the effectiveness of the differential pumping capacity through a helium partial pressure measurement using a quadrupole mass spectrometer at the plasma vacuum chamber. The propellant gas (He) inflow rate into the chamber is below the measurable limit under background conditions at 10^{-7} Pa helium partial pressure, and this value is consistent with the calculated value.

3.4 Demonstration of injection timing control system

Pellet injection control is performed based on the previously set sequence in synchronization with the LHD central control system. A block diagram of the repetitive pellet injector is shown in Fig. 10. The repetitive pellet injector is mainly controlled by the two programmable logic controllers (PLC), which are remotely operated by a Windows-based control PC in the control room via a TCP/IP network. For pellet injection timing control, injection timing triggers are generated by a 1 kHz pulse generator card and a fast counter card, which are mounted on a PCI-compliant slot in the control PC. There are two injection timing control modes: a pre-program mode and a density-control mode. In the pre-program mode, pellets are injected based on the previously set injection timings. We can set the injection timing on the millisecond time scale unless the time interval between injections is below $t_{\text{min}} = 90$ ms, which corresponds to the upper limit of the injection frequency. In the density-control mode, injection timing is determined by comparing the target value and measured density signal (\bar{n}_e), as shown in Fig. 11. The density gate signal becomes logical-high when the measured density signal is lower than the target value. The injection gate signal that is

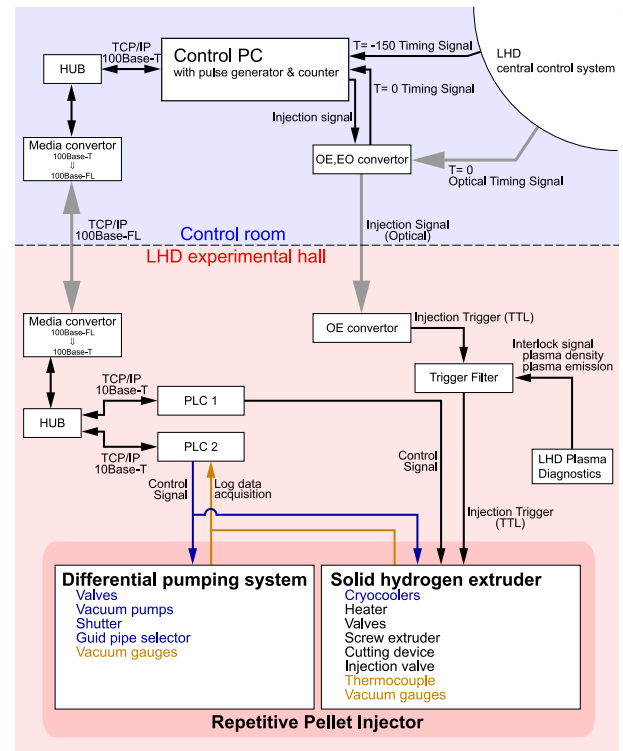


Fig. 10 Block diagram of the repetitive pellet injector control system.

normally logical-high becomes logical-low during t_{min} just after pellet injection, in order to prevent high frequency injection over the upper limit of the injection frequency. The pellet injection trigger is produced by the logical product of the density gate signal and injection gate signal.

Density control experiments using abovementioned control method were performed in LHD, which is an excellent platform to examine pellet injector performance due to the steady state capability and high density adaptability. The line average density waveforms of the density controlled discharges are shown in Fig. 12. Quasi-constant density control in the range from $0.4 \times 10^{20} \text{ m}^{-3}$ to $1.0 \times 10^{20} \text{ m}^{-3}$ and ramp-up density control were demonstrated successfully. Repetitive pellet injection contributes in maintaining not only high-density plasma but also in achieving good confinement in the high-density regime, which can not be attained by gas puff fueling [23]. Although the repetitive pellet injector can provide pellets without any restriction, the discharge duration is limited by the pulse length of the NBI heating and/or pumping capacity necessary to prevent radiation collapse due to excess neutral gas.

Repetitive pellet injection is also effective for minority hydrogen ion fueling into the helium dominated plasma in ICRF long pulse discharge with a minority heating scenario [24]. In order to perform the ICRF minority heating, adequate control of the minority hydrogen ions is required. In the case of gas puff fueling, it is difficult to control a

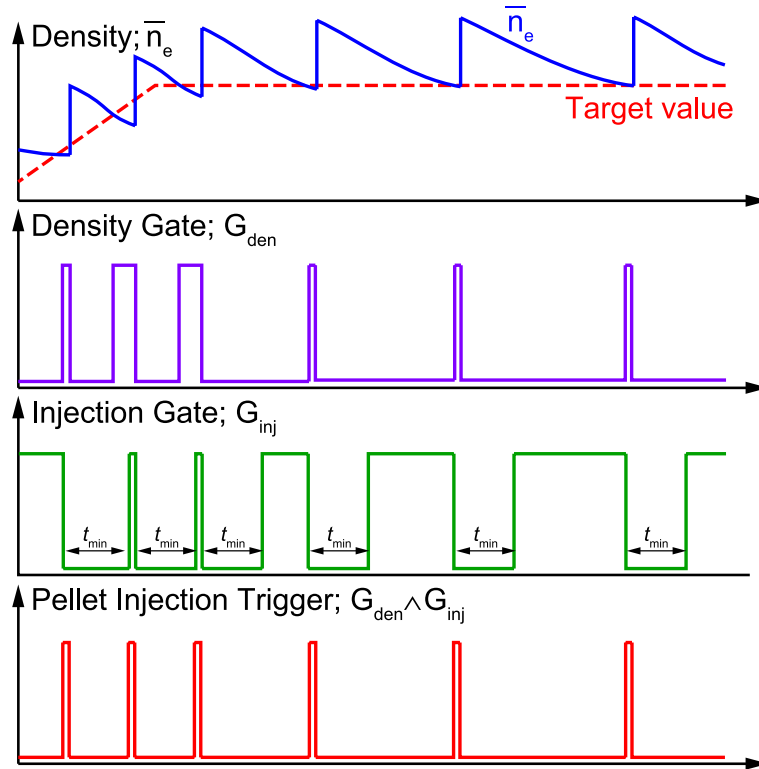


Fig. 11 Timing chart of the real-time pellet injection timing control.

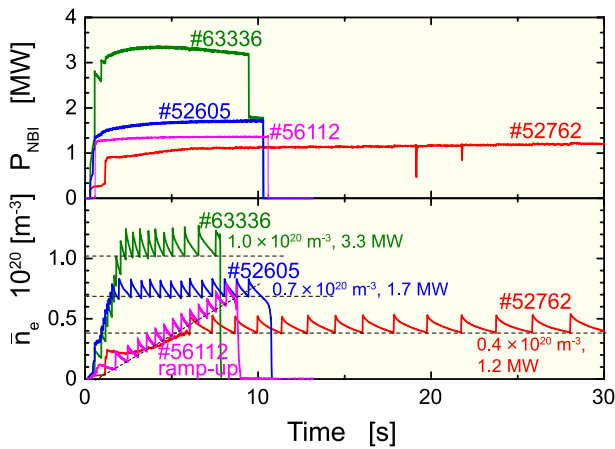


Fig. 12 Time evolution of electron density with real-time pellet injection timing control.

small amount of hydrogen ions in the plasma confinement region because the fueling property is ruled by a recycling process that is carried out outside the plasma confinement region. On the other hand, repetitive pellet injection can control the minority hydrogen ratio in the confinement region directly. Figure 13 shows a typical waveform of the ICRF heated long pulse discharge with minority hydrogen fueling by pellet injection. To maintain a low level minority ratio, very small pellets (less than 10% of rated size) were injected by reducing the solid hydrogen extru-

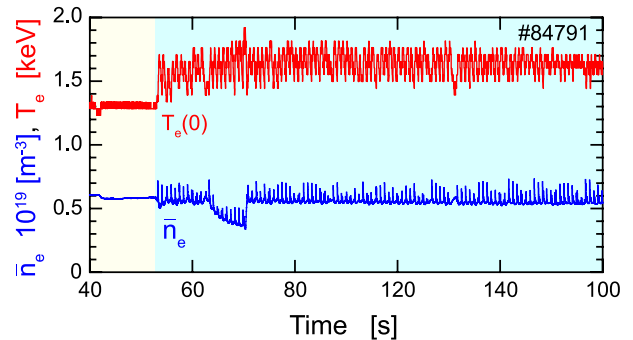


Fig. 13 Time evolution of the electron density and temperature in ICRF heated long pulse discharge with minority hydrogen fueling by pellet injection. Repetitive pellet injection starts at 53 s.

sion speed with a high injection frequency (5 ~ 10 Hz). The typical density rise per pellet is about $2 \times 10^{18} \text{ m}^{-3}$. The effective minority hydrogen fueling by repetitive pellet injection improves the ICRF heating efficiency compared with gas puff fueling and leads to an increase in electron temperature. Since pellet injection fueling can control the plasma fuel ratio in the confinement region directly as demonstrated above, it has a potential for core fueling by controlling the D/T fuel ratio in a future fusion reactor, where usage of the tritium should be minimized.

4. Summary

Two types of solid hydrogen pellet injection systems have been developed at the National Institute for Fusion Science. One is an *in-situ* pipe-gun type pellet injector, which is the simplest of all pellet injectors. The other is a repetitive pellet injector with a screw extruder. The screw extruder can form 3.0 mm ϕ solid hydrogen rod continuously at extrusion rates of \sim 55 mm/s, and this feature allows consecutive pellet injection. The repetitive pellet injector is the first pellet injector, which has steady-state injection capability for plasma experiments. Both pellet injectors employ compact cryo-coolers to solidify hydrogen; therefore, both can be operated with just an electrical input instead of a liquid helium supply system. These effective pellet injectors have demonstrated stable operation during the past 11 years in LHD experiments.

The repetitive pellet injector represents a step toward future reliable steady-state refueling of a fusion reactor. Future prospects of the pellet injection for plasma fueling can be forecast, but there are issues that need to be addressed for future reactors. One is an on-demand solid hydrogen extrusion control for controlling pellet characteristics such as pellet size, D/T fuel ratio, and injection frequency in real time. Another is alternative pellet acceleration that can attain higher speeds with lower propellant gas consumption in term of the reduction in tritium utilization.

Acknowledgment

The authors would like to thank Dr. I. Viniar for his support to the development of the repetitive pellet injector. We also would like to thank Dr. L.R. Baylor, Dr. S.K.

Combs, Dr. P.W. Fisher, Dr. S.L. Milora and Dr. P.T. Lang for their contribution and communication. This work is supported by NIFSULPP521, NIFSULPP522 and Grant-in-Aid for Scientific Research (A)13358006.

- [1] S.L. Milora, Nucl. Fusion **35**, 657 (1995).
- [2] B. Pégourié, Plasma Phys. Control. Fusion **49**, R87 (2007).
- [3] S.K. Combs, Rev. Sci. Instrum. **64**, 1679 (1993).
- [4] J. Urbahn *et al.*, Proceedings of 15th Symposium on Fusion Engineering Vol. **1**, 44 (1993).
- [5] S.K. Combs *et al.*, Rev. Sci. Instrum. **60**, 2697 (1989).
- [6] C. Andelfinger *et al.*, Rev. Sci. Instrum. **64**, 983 (1993).
- [7] S.K. Combs *et al.*, Rev. Sci. Instrum. **66**, 2736 (1995).
- [8] Y. Oda *et al.*, Vacuum **41**, 1510 (1990).
- [9] K. Kizu *et al.*, Fusion Sci. Technol. **42**, 396 (2002).
- [10] H. Yamada *et al.*, Fusion Eng. Des. **49-50**, 915 (2000).
- [11] H. Yamada *et al.*, Fusion Eng. Des. **69**, 11 (2003).
- [12] P.C. Souers, *Hydrogen properties for fusion energy* (Berkeley : University of California Press, 1986).
- [13] J. Lafferranderie *et al.*, Proceedings of 14th Symposium on Fusion Technology Vol. **2**, 1367 (1986).
- [14] R. Sakamoto *et al.*, Nucl. Fusion **41**, 381 (2001).
- [15] R. Sakamoto *et al.*, Plasma Fusion Res. **2**, 047 (2007).
- [16] S.K. Combs *et al.*, Rev. Sci. Instrum. **56**, 1173 (1985).
- [17] Y. Oda *et al.*, Proceedings of 18th Symposium on Fusion Technology Vol. **1**, 661 (1994).
- [18] I. Viniar *et al.*, Instrum. Exp. Tech. **43**, 722 (2000).
- [19] I. Viniar *et al.*, Fusion Eng. Des. **58-59**, 295 (2001).
- [20] L.R. Baylor *et al.*, Phys. Plasmas **12**, 056103 (2005).
- [21] L.R. Baylor *et al.*, Nucl. Fusion **47**, 443 (2007).
- [22] L.D. Landau and E.M. Lifshitz, *Fluid mechanics* (Pergamon Press, 1987).
- [23] R. Sakamoto *et al.*, Nucl. Fusion **46**, 884 (2006).
- [24] T. Seki *et al.*, AIP Conf. Proc. **787**, 98 (2005).